SUPPLEMENTARY MATERIAL 1

TOWARDS THE RECONCILIATION OF VISCOSITY CHANGE AND CO_2-INDUCED POLYMERIZATION IN SILICATE MELTS

Yann MORIZET[1], Michael PARIS[2], David SIFRE[3], Ida DI CARLO[3], Sandra ORY[4], Fabrice GAILLARD[3]

[1] Université de Nantes, Nantes Atlantique Universités, Laboratoire de Planétologie et Géodynamique de Nantes (LPG), UMR CNRS 6112, 2 rue de la Houssinière, 44322 NANTES (France)

[2] Institut des Matériaux Jean Rouxel (IMN), Université de Nantes, UMR CNRS 6502, 2 rue de la Houssinière, BP32229, 44322 NANTES Cedex 3 (France)

[3] CNRS/INSU-Université d'Orléans – BRGM, UMR 7327, Institut des Sciences de la Terre d'Orléans, 1A rue de la Férollerie, 45071, Orléans, France

[4] CNRS-CEMHTI Conditions Extrêmes et Matériaux: Haute Température et Irradiation, UPR 3079, 1D avenue de la Recherche Scientifique, 45071, Orléans, France

1. CO_2 content determination

We used the method described by Morizet et al. (2013) to determine the CO_2 content via Raman spectroscopy. This Raman calibration for CO_2 content is a linear calibration function such as wt.% CO_2 = 15.17 x CO_3/HF relating the CO_2 content to the ratio between the area of the CO_3^{2-} peak and the high frequency envelop of the silicate glass vibrational signature

(CO_3/HF). The calibration was established from a database on CO_2-bearing silicate glasses (65 data points) with CO_2 up to ~16 wt.% CO_2. We extended this Raman calibration to additional CO_2 content data (89 data points) with higher CO_2 content (up to 23 wt.% CO_2) determined using bulk analyzer (Figure S1). The entire dataset for this calibration is provided in the Supplementary material 2 as a spreadsheet. The calibration function has been modified according to this new database and the linear relationship is wt.% CO_2 = 13.5 x CO_3/HF; where HF stands for the high-frequency of the symmetric stretch of the aluminosilicate network. Using this method, the typical error on the CO_2 content is 10% in relative to the value. We made an analysis of the typical error with the updated database. In Figure S1, we added the error dispersion lines as reported by the fit. The standard deviation on the CO_3/HF ratio is 0.125 and the r^2 parameter is 0.969. As a result, for a CO_3/HF = 1.25, the error is 10% in relative to the value; it will be lower than 10% at higher CO_3/HF and higher than 10% at lower CO_3/HF. Considering the dispersion of the data points in Figure S1, we definitely think this cannot be the truth: we observe that the scattering of the data point at low CO_3/HF ratio is small and on the contrary is more important at high CO_3/HF ratio. In order to be on the safe side, we consider a 10% error in relative to the value for the whole range of CO_3/HF ratio determination.

We show in Figure S2 a comparison of the CO_2 content determination using Raman spectroscopy and EPMA shortfall. This latter approach has been commonly used to estimate CO_2 content dissolved in silicate glasses (Dasgupta et al., 2007; Moussallam et al., 2015); however, the accuracy in the determination of the CO_2 content is low (error above 20% in relative to the value as reported by Dasgupta et al., 2007). The corresponding data are provided in Table 1. In Figure S2, the wt.% CO_2 by EPMA is calculated using the difference to 100% from the major element analyses and corrected by the H_2O content determined by FTIR spectroscopy. We observe in Figure S2 that the data points except for RB8E-13 are

aligned along the 1:1 line suggesting that the Raman calibration method is accurate enough to determine the CO_2 solubility in the present investigated glasses.

The typical deconvolution of the Raman spectra for the CO_2-bearing glasses is shown in Figure S3. We report the deconvolution for several samples with CO_2 ranging from 6.2 (RB8E-6) to 18.0 wt.% (RB8E-11). On each spectrum, we added the derived CO_3/HF ratio from the area of the peaks as well as the calculated CO_2 content using the calibration factor of 13.5 mentioned earlier. We should emphasize that such approach is only one possible solution; however, there is a clear definition of the ν_1 CO_3^{2-} peak at 1075 cm^{-1}, hence any variation in the deconvolution would not induce strong variation in the CO_3/HF ratio and therefore in the derived CO_2 content. The entire set of simulation parameters is provided in Supplementary material 2.

2. Change in ^{17}O species as a function of CO_2 content

We present in Figure S4 the change in the O species abundances as a function of XCO_2 as determined from Raman spectroscopy (see Table 1). The O species concentrations were determined from the ^{17}O NMR spectra simulations shown in Figure 1B. We clearly observe as the XCO_2 increases that there is a gradual increase in the abundance of bridging oxygens species (BO), whereas in the same time the concentration of non-bridging oxygens (NBO) decreases. These opposite trends are consistent with the identified effect of CO_2 towards an increase in the degree of polymerization of the silicate melt structure.

The concentration of the oxygen triclusters (O^{III}) does not seem to change as a function of CO_2 content, however, due to the low abundance of the O^{III} identifying any fluctuation would be unwise. The peak identified at ~+150 ppm in the ^{17}O NMR spectra has been attributed to

the signature of ^{17}O nuclei in CO_3^{2-} dissolved within the glass structure. This peak appears to increase with increasing CO_2 content with an increasing factor very close to 1. Similar chemical shift is also mentioned in early work (Klemperer, 1978) which reports a ^{17}O chemical shift ranging from +100 to +180 ppm for carbonate groups in organic compounds.

3. Change in NBO/T as a function of CO_2 content

In the main text (see Figure 2), we report the deviation in the NBO/T (ΔNBO/T) as a function of CO_2 content calculated as the molar fraction (XCO_2). In Figure S5, we show the actual change in the NBO/T measured by ^{17}O and ^{29}Si NMR spectroscopy as a function of the XCO_2. As expected, the observed change in the NBO/T from ^{17}O and ^{29}Si NMR corroborates the drawn conclusions in the main text: 1) the measured NBO/T from ^{17}O and ^{29}Si NMR is higher than the one obtained from stoichiometric calculation indicating an excess NBOs concentration (NBO/T > 2 at $XCO_2 = 0$); 2) CO_2 induces a polymerization of the silicate melt structure; 3) the induced polymerization is much more important than the predicted polymerization from the theoretical dissolution mechanism (see Eq. 1). For this latter point, we derived in Figure S5A and B a slope of -3.1 and -3.2 for ^{17}O and ^{29}Si NMR results, respectively; in comparison to the slope of -2 following the dissolution mechanism of Eq. 1.

References Supplementary material 1:

Dasgupta, R., Hirschmann, M.M., Smith, N.D., 2007. Partial melting experiments of peridotite + CO_2 at 3 GPa and genesis of alkalic ocean island basalts. J. Petrol. 48, 2093–2124.

97 Klemperer, W.G., 1978. ^{17}O-NMR spectroscopy as a structural probe. Angew. Chem. Int.
98 Engl. 17, 246–254.

99

Supplementary Figures:

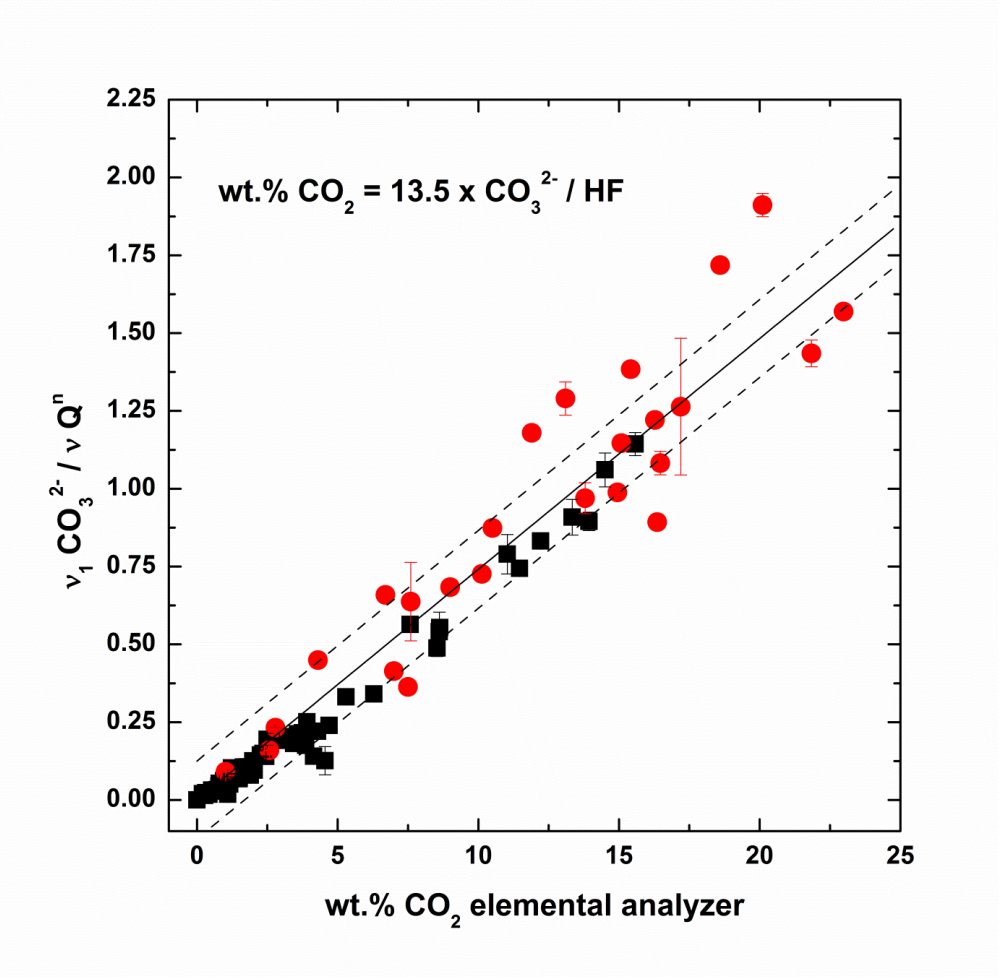

Figure S1: Calibration for CO_2 content in silicate glasses using Raman spectroscopy. This calibration represents an updated version of the one proposed by Morizet et al. (2013) based on 65 data points and for CO_2 content up to 16 wt.%. The new calibration is based on 89 data points and for CO_2 content up to 23 wt.% in silicate glasses (see Supplementary material 2 for the entire dataset). The dashed lines represent the 95% confidence interval. The r^2 of the linear regression is 0.969.

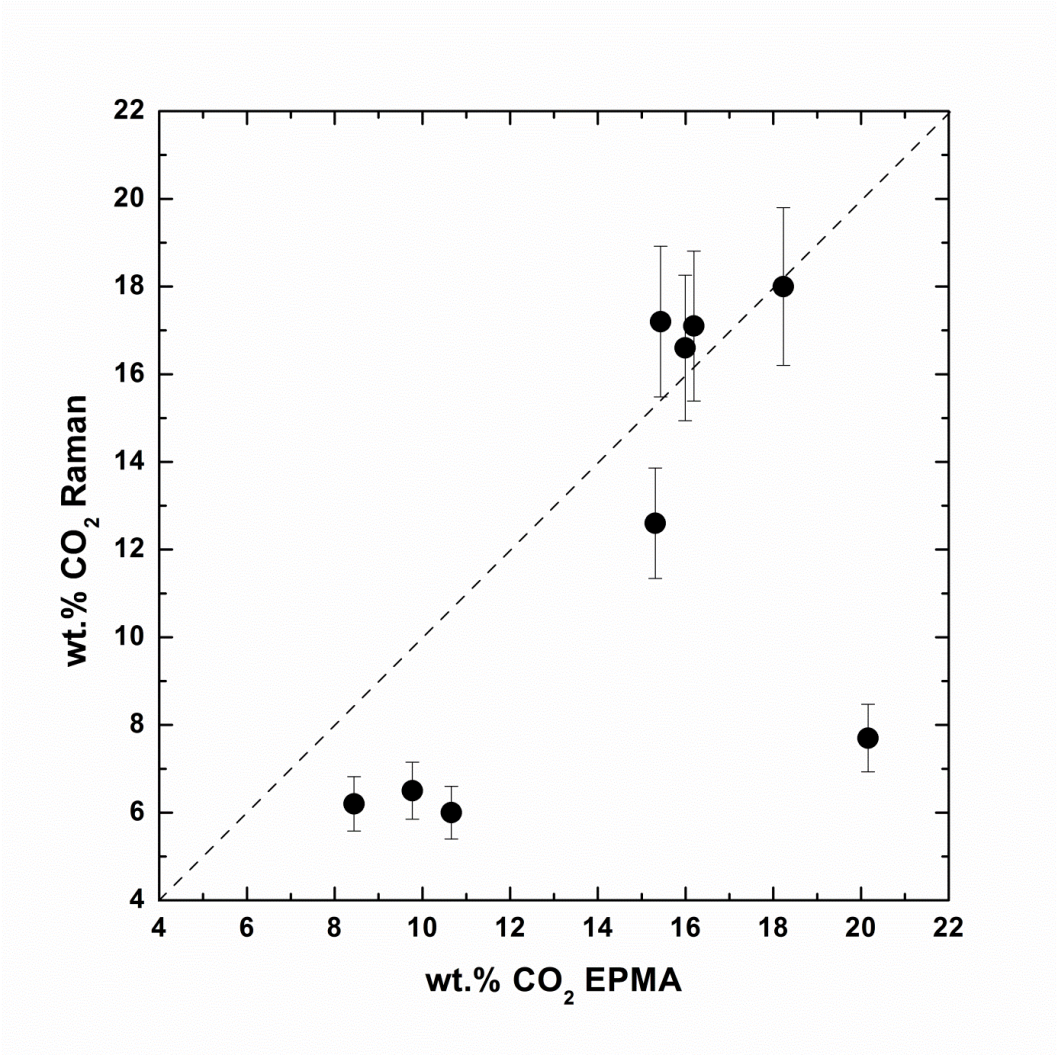

Figure S2: wt.% CO_2 determined by Raman versus wt.% CO_2 estimated from the EPMA shortfall. The EPMA shortfall represents the difference to 100% in the major element concentration (see Table 1). The EPMA shortfall is corrected by the H_2O content determined by FTIR to extract the CO_2 content. No error is reported for the CO_2 content determined by EPMA as this method leads to high uncertainty (see the outlier at 20 wt.% CO_2 from EPMA and 8 wt.% CO_2 from Raman).

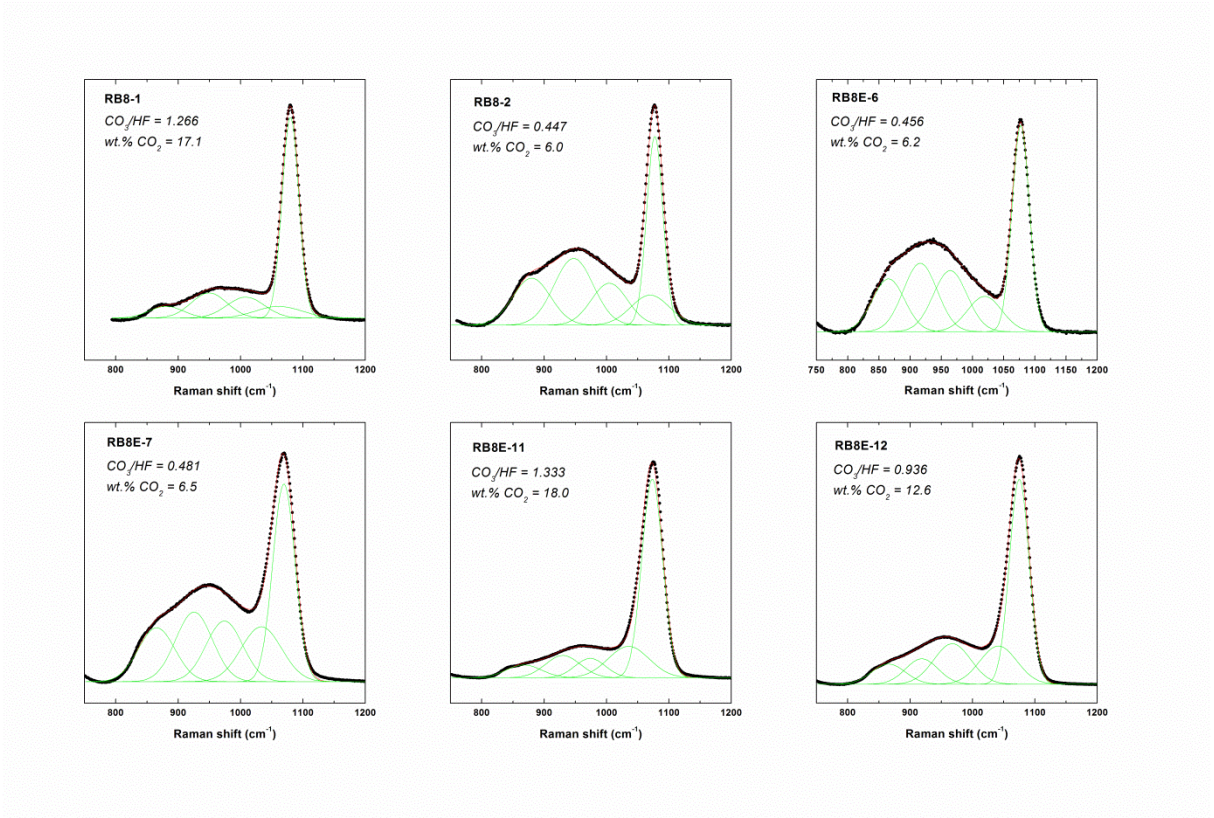

Figure S3: Glass sample Raman spectra simulated with five Gaussian lines corresponding to the symmetric stretch of the CO_3^{2-} group (ν_1 CO_3^{2-}) and silicate network (ν_1 Q^n). The simulation is reported for RB8 and RB8E samples. The ratio CO_3/HF is reported next to each simulation and is used to calculate the CO_2 content from the linear correlation (see text for detailed discussion).

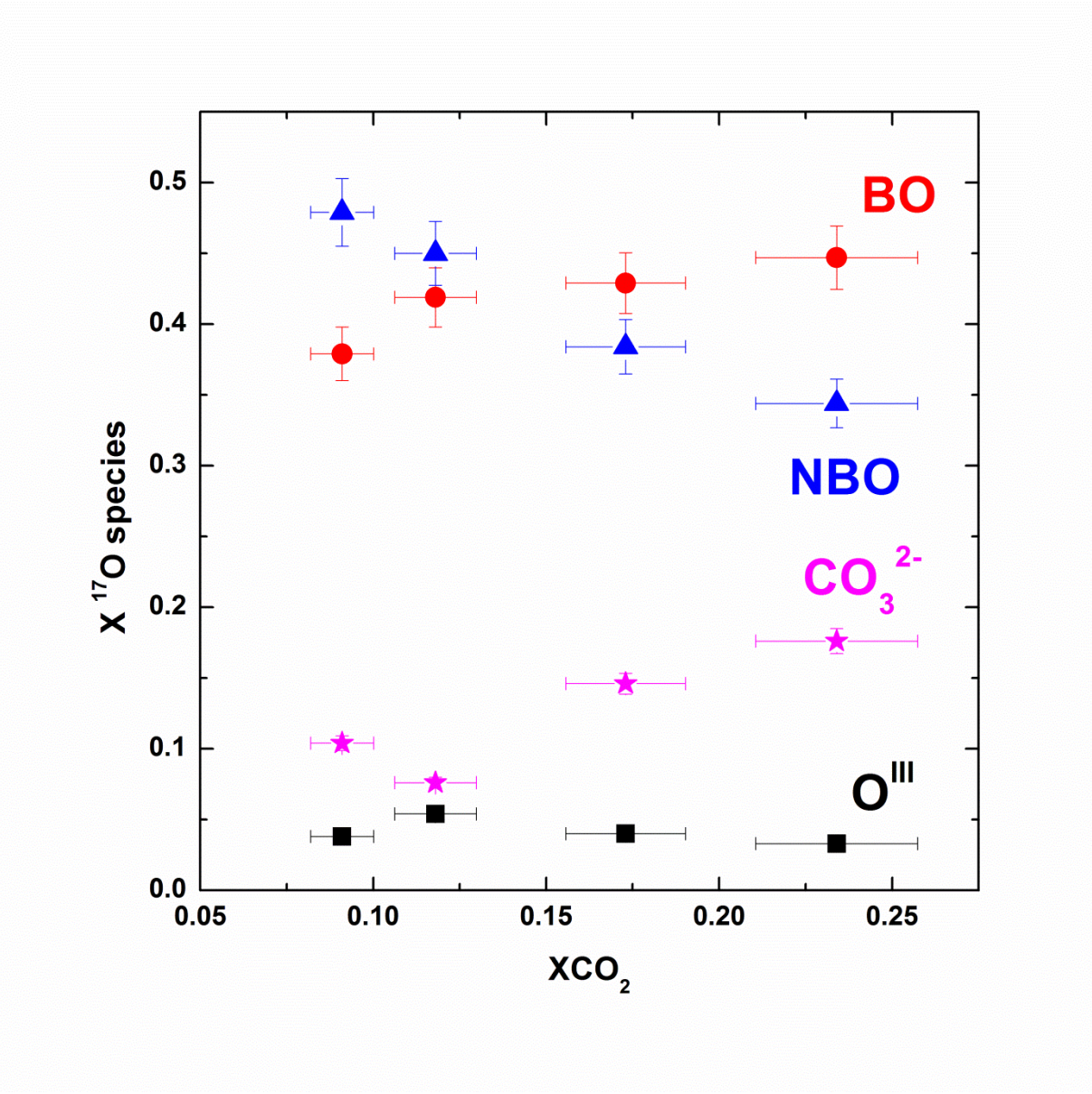

Figure S4: Distribution of ^{17}O species as a function of XCO_2. The XCO_2 was determined from the Raman simulation results given in Table 1 and using the major element concentrations obtained from EPMA analyses. The molar fraction of the ^{17}O species was obtained from the simulation of the ^{17}O NMR spectra shown in Figure 1B of the manuscript main text.

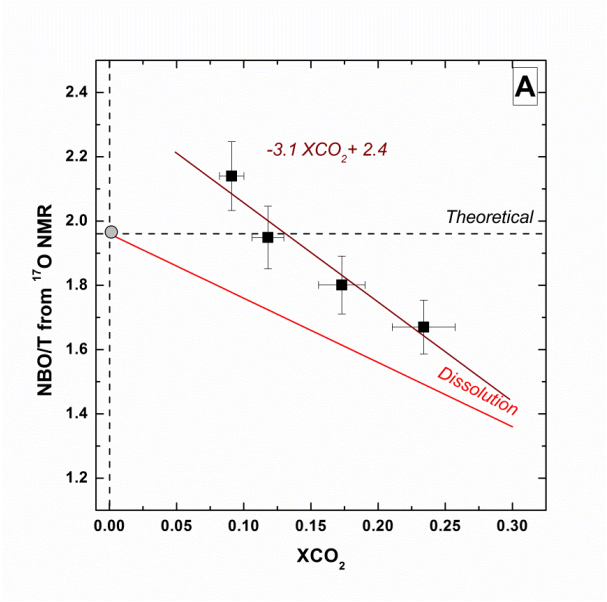

131

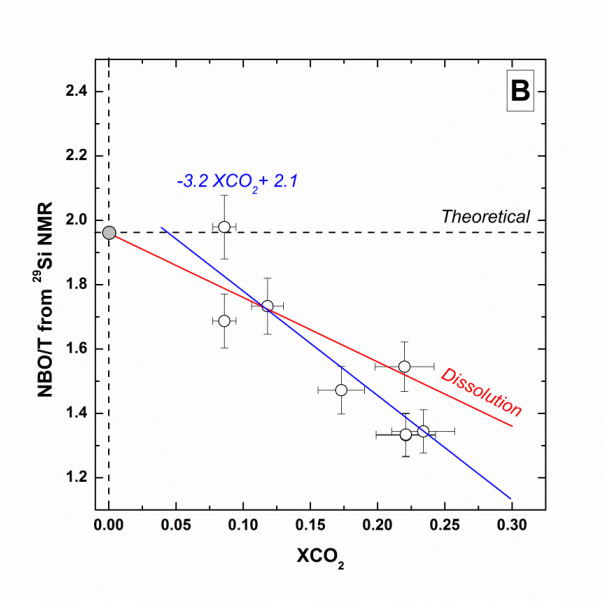

132

133 Figure S5: Change in the degree of polymerization (NBO/T) determined from ^{17}O (A) and
134 ^{29}Si (B) NMR as a function of XCO_2 (see Table 2). Line corresponding to the theoretical
135 degree of polymerization (1.96, see Table 1) is shown. Line corresponding to the change in
136 the degree of polymerization following the Eq. 1 dissolution mechanism is reported. On each
137 plot, we added the linear regression for ^{29}Si and ^{17}O NMR data points.

138